REMOVAL OF ARSENIC IN GROUNDWATER USING NOVEL MESOPOROUS SORBENT

CIVIL AND ENVIRONMENTAL ENGINEERING (ENVIRONMENTAL PROGRAM)

UNIVERSITY OF WISCONSIN-MADISON

2003

This project was supported, in part, by General Purpose Revenue funds of the State of Wisconsin to the University of Wisconsin System for the performance of research on groundwater quality and quantity. Selection of projects was conducted on a competitive basis through a joint solicitation from the University and the Wisconsin Departments of Natural Resources; Agriculture, Trade and Consumer Protection; Commerce; and advice of the Wisconsin Groundwater Research Advisory Council and with the concurrence of the Wisconsin Groundwater Coordinating Council.

Table of Contents

List of Figures

List of Tables

PROJECT SUMMARY

PROJECT ID: R/UW-REM-006

INVESTIGATOR:

PRINCIPAL INVESTIGATOR: JAE K. PARK, PROFESSOR, CEE

RESEARCH ASSISTANT: MIN JANG, PhD, CEE

PERIOD OF CONTRACT: 7/01/2002~6/30/2003

BACKGROUND/NEED:

Through our batch tests, we found that this technique will be effectively applied for arsenic removal from groundwater. However, it is needed to conduct experimental works with a real groundwater contaminated arsenic species in order to design the POU/POE application of arsenic removal.

OBJECTIVES:

The objectives of this study were as follows: (1) to develop novel adsorbents through synthesizing highly ordered mesoporous silica SBA-15 and incorporating lanthanum oxide using an incipient-wetness impregnation technique; (2) to characterize the physicochemical properties of these media using several fine characterization techniques such as; XRD, N_2 gas *isotherm* analysis, and FTIR; (3) to evaluate the adsorption capacities through performing adsorption *kinetics* and *isotherms* of arsenate; and finally (4) to try to elucidate the adsorption behavior of the media in connection with the physicochemical characterization discovered by above fine tools.

METHODS:

Preparations of experimental procedure: Environmental Program Lab. (July/02~June/03)

Kinetics and isotherms: Environmental Program Lab. (Sep/02~May/03)

Analysis of physicochemical properties of media (Sep/02~June/03)

XRD: Materials Science and Engineering

N_2 gas isotherms: Water Chemistry

FTIR: Forest Product Lab.

HRTEM: Materials Science and Engineering

XPS: Materials Science and Engineering

Surface complexation modeling: Environmental Program Lab. (Jan/03~March/03)

RESULTS AND DISCUSSION:

XRD and N_2 *isotherm* results showed that an immoderate substitution of lanthanum into silica networks was occurred at 80 percent of lanthanum impregnation even though lanthanum was highly dispersed into the mesopore structures of SBA-15 without a formation of lanthanum oxide particles.

FTIR results showed that there was no structural collapse of silica frameworks at 80 percent lanthanum impregnation. This can be explained as a result of a partial substitution of lanthanum precursors with silicon, which could play an important role in structural stabilization as has been shown by other studies.

Although the arsenate adsorption densities increased with lanthanum impregnation up to 50% (the most efficient percentage of lanthanum impregnation), it abruptly decreased at 80% due to the substitution of lanthanum with silicon, leading to the overall reduction of arsenate adsorption capacity.

At the arsenate concentration of 0.667 $mmol_{As}/L$ in this study, the adsorption capacity of 50% lanthanum-impregnated SBA-15 (designated to La_{50}SBA-15) was 1.651 $mmol_{As}/g$, (123.7 mg_{As}/g) which was about 10 or 14 times higher than the other referenced values of La(III) impregnated alumina (0.172 $mmol_{As}/g$) or La(III) impregnated silica gel (0.118 $mmol_{As}/g$).

CONCLUSIONS/IMPLICATIONS/RECOMMENDATIONS:

Nano-scale impregnation of lanthanum onto SBA-15 has a lot of advantages in terms of not only adsorption velocity and capacity but also cost benefits for small scale of POU/POE application of arsenate removal since a small amount of lanthanum precursor is needed for impregnation and the regeneration of the lanthanum-impregnated mesoporous media will be applicable due to excellent structural stability of lanthanum-impregnated SBA-15.

RELATED PUBLICATION:

SCI Paper

(1) Min Jang, Eun Woo Shin, Jae K. Park, and Sang I. Choi, Mechanisms of Arsenate Adsorption by Highly-Ordered Nano-Structured Silicate Media Impregnated with Metal Oxides, Accepted in *Environmental Science and Technology* (August 28, 2003).

(2) Min Jang, Park, Jae K., Eun Woo Shin, Lanthanum Functionalized Highly Ordered Mesoporous Media for Arsenic Removal, Submitted to *Environmental Science and Technology*.

US Patent

Jae K. Park and Min Jang, "Removal of Arsenic and Other Anions Using Novel Adsorbents," Patent (U.S. Patent) proceeding.

Presentation

Min Jang, Eun Woo Shin, and Jae K. Park, Removal of Arsenic Using Mesoporous Silicate Media Impregnated Metal Oxides Nano-Particles, WEFTEC, Research Section 41, Chicago.

KEY WORDS: arsenic, mesoporous, SBA-15, lanthanum, adsorption

FUNDINGS: the State of Wisconsin Groundwater Research Program through the University of Wisconsin Water Resources Institute (WRI)

1.1 INTRODUCTION

As a medium having higher sorption capacity than activated alumina, lanthanum oxide has higher isoelectric point (IEP) of 11.1 than activated alumina (9.2) (Misra and Nayak, 1995). It is also one of the cheapest rare-earth elements, is extracted from bastnaesite and monazite (Tokunaga *et al.*, 1999b), and has been known as nontoxic and environmental friendly (Tokunaga *et al.*, 1999a). For these reasons, many researchers have investigated the precipitation and/or adsorption processes (Wasay *et al.*, 1996a; Tokunaga *et al.*, 1997) using lanthanum compounds for the removal of oxyanions such as selenium and arsenic species. Wasay *et al*. (1996a and 1996b) studied the adsorption process of a lanthanum-impregnated silica gel and La(III)-impregnated alumina to remove fluoride, phosphate, selenite, and arsenate ions. A wet impregnation method was used to incorporate lanthanum ions on the surface functional groups. Their adsorption *isotherm* results showed that the adsorption of each anion followed the *Langmuir isotherm* without interferences of other anions such as Cl^-, Br^-, I^-, NO_3^-, and SO_4^{2-}.

Up to now, using the characteristics of mesoporous materials, there has been a great deal of some efforts to develop several types of adsorbents for removal of arsenic or other toxic elements. Fryxell *et al.*, synthesized copper chelated ethylenediamine (EDA) immobilized mesoporous silicate as anion adsorbent. In their synthesis procedure, they used the mesitylene organic solution to expand pore structures and cetyltrimethylammonium chloride/hydroxide as pore templating agent (Fryxell *et al.*, 1999). After grafting the ethylenediamine (EDA) silane onto the surface of mesoporous silica, Cu (II) ions were bonded to create octahedral complexes. Their media had positively charged hosts with three-fold symmetry which match the geometry of tetrahedral anions, so that they showed high selectivity of anions as well as high sorption capacity of about 140 mg (arsenate)/g. Yoshitake *et al.*, attempted to synthesize several types of cations (Fe^{3+}, Co^{2+}, Ni^{2+}, Cu^{2+}, and H^+) coordinated aminosilane-functionalized MCM-41, SBA-1, and MCM-48, inspecting the arsenate adsorption properties (Yoshitake *et al.*, 2002; Yoshitake *et al.*, 2003). They found that Fe/NN-MCM-41 had a distribution coefficient of more than 2.0×10^5 even at below 100 mg/L of arsenate concentration and showed the highest arsenate adsorption capacity of 2.5 $mmol_{As}/g$. However, as described above, both cases tried to utilize complicated synthesis procedures, in which expensive and toxic chemicals were used, resulting in a significant limitation for a large-scale application. Accordingly, in this study, simplified and economic synthesis routes of adsorbents, which still have high adsorption capacities of anionic toxic species, were investigated. Using amphiphilic triblock copolymers as a structure-directing template agent, the mesoporous silica molecular sieves SBA-15 were successfully synthesized under hydrothermal conditions (Zhao *et al.*, 1998). The uniform two dimesional hexagonal (space group *p6mm*) mesopore channels of SBA-15 can be tailored by changing synthesis conditions. The objectives of this study were as follows: (1) to develop novel adsorbents through synthesizing highly ordered mesoporous silica (SBA-15) and incorporating lanthanum oxide using an incipient-wetness impregnation technique; (2) to characterize the physicochemical properties of these media using several fine characterization techniques, such as XRD, N_2 gas *isotherm* analysis, and FTIR, (3) to evaluate the adsorption capacities through performing adsorption *kinetics* and *isotherms* of arsenate; and finally (4) to try to elucidate the adsorption behavior of the media in connections with the physicochemical characterization discovered by above fine tools.

1.2 PROCEDURES AND METHODS

Synthesis of lanthanum-impregnated SBA-15 and conductivity tests

SBA-15 was synthesized using triblock copolymer (Pluronic P123, $EO_{20}PO_{70}EO_{20}$, Aldrich®) as a structure-directing reagent and tetraethyl orthosilicate (Aldrich®) as a silica precursor. A 4-gram triblock copolymer was dissolved in 60 mL of deionized water for 30 min and a 2 M hydrochloric acid solution was added. The mixed solution was stirred for 30 minutes. Tetraethyl orthosilicate (TEOS) was then added to the mixture and heated at 35°C for 20 hrs. The mixture was transferred into a Teflon bottle and heated at 90°C for 24 hrs without stirring. The solid product was then filtered with a 0.45-μm filter paper and dried at room temperature under vacuum before calcination. The mole fraction of each component for as-synthesized SBA-15 was 1 mol TEOS: 5.854 mol HCl: 162.681 mol H_2O: 0.0168 mol triblock copolymer. The calcination was performed in an oven at 550°C for 6 hrs in air to remove the triblock copolymer organic component. The calcined SBA-15 was preserved at room temperature under vacuum. $La(NO_3)_3 \cdot xH_2O$ (x = 3~5, Aldrich®) was selected as lanthanum precursor to incorporate into SBA-15 through use of an incipient wetness impregnation technique (Jang *et al.*, 2003). The mixture was dried in the hood at room temperature for 1 day. To compare the IR spectra, lanthanum oxide was synthesized by the same lanthanum precursor with the following procedure. A 100 mL solution of lanthanum precursor was prepared with a concentration of 3 $mole_{La}$/L of deionized water. The solution was then dried in an oven at 105°C for one day. All solids were then calcined in an oven at the programmed temperature of the range starting from room temperature to 550°C at a rate of 0.5°C per minute, and preserved for 4 hours. After calcinations, the solids were kept inside a vacuum chamber.

In order to find the optimum temperature for completing the oxidation of lanthanum precursors, calcinations was conducted with different temperatures, followed by conductivity test. The SBA-15 impregnated with highest impregnated percentage (80%) of lanthanum precursor was calcined in an oven at the programmed temperature of the range from room to planned temperatures at a rate of 0.5°C/min. The solids were then calcined at final temperature for 4 hours. After calcination, solids were kept on a vacuum chamber before conductivity tests. The conductivity tests were conducted according to the procedure described by Jang *et al*, (2003).

Characterization of LaSBA-15

A Stoe High Resolution X-Ray Diffractometer (Microphotonics, Allentown, Pa.) equipped with Cu Kα radiation (40 kV, 25 mA) was used to obtain x-ray diffraction patterns in a short range (0.8°~2.1°) for a series of lanthanum-impregnated SBA-15 and calcined SBA-15. A wide range (10°~70°) of x-ray diffraction pattern was conducted for La_{80}SBA-15, which has the largest portion of lanthanum (44.4 percent) based on the mass of media. N_2 gas adsorption-desorption *isotherms* were performed at 77 K using a Micromeritics ASAP 2400 analyzer (Norcross, Ga.). Media were dehydrated at 393 K for 1 day before performing *isotherm* tests. The BET specific surface area (A_{BET}) was calculated by the linear part of the BET equation in the range of relative pressure range from 0.05 to 0.2. The primary mesopore size distributions (PSD) of media were obtained using Barrett, Joyner and Halenda (BJH) method with the corrected Kelvin equation of the adsorption branch of the hysteresis loop of the nitrogen adsorption *isotherm*, which can accurately calculate pore size distribution under the assumption of a cylindrical shape of pores (Kruk and Jaroniec, 1997; Newalkar *et al.*, 2001a; Newalkar *et*

al., 2001b). The pore diameter corresponding to the maximum of PSD is denoted as W_{KJS}. The primary mesopore (V_p) was estimated using the β_s plot method, which is an easily determined alternative to α_s plot method ($\alpha_s = v_{ads}\ (P/P_0)/v_{ads}\ (0.4)$). Based on Frenkel, Halsey and Hill (FHH) theory, the v_{ads} of α_s equation is replaced by the statistical thickness of the adsorbed gas layer to have a following equation: $\beta_s = [\ln(0.4)/\ln(P/P_0)]^{(1/2.7)}$ (Lukens *et al.*, 1999). Micropore volume (V_{micro}) and area (A_{micro}) were obtained by *t*-plot method. The total pore volumes (V_t) were determined at 0.99 of relative pressure. IR spectra were obtained by a Mattson Galaxy 5020 FTIR spectrometer (Mattson Instruments, Madison, Wis.) to get the information of the change of functional groups onto the oxide surface and structural stability after lanthanum impregnation at room temperature. Potassium bromide was used to mix with samples.

Arsenate Adsorption *Kinetic* Tests

Sodium arsenate ($Na_2HAsO_4{\cdot}7H_2O$, Sigma®) was used as the arsenate source for a stock solution without any modification. A stock solution of arsenate (133 mmol/L) was prepared with 0.01 *M* $NaNO_3$ solution based on deionized water. A Photronix® reagent grade water system was used to prepare all of deionized water. Granular activated alumina (AA-400G, ALCAN®, 8×14 mesh) was selected as a commercialized product for arsenic removal to compare the adsorption *isotherm* and *kinetic* data with various amounts of lanthanum-impregnated SBA-15. The specific surface area of activated alumina was 350~380 m^2/g (ALCAN, 1997).

Arsenate *kinetic* studies were conducted with various amounts of lanthanum-impregnated SBA-15 and granular activated alumina. An aliquot of 1,000 mL of deionized water prepared with 0.01 *M* $NaNO_3$ was poured into a reaction bottle for each *kinetic* study. After adding arsenate stock solution to make the initial arsenate concentration of 0.267 $mmol_{As}/L$, the solution was stirred with a magnetic stirrer at a velocity of 500 rpm. The pH of the solution was adjusted to 7.2±0.02 with an automatic pH titrator and the temperature was maintained at 20±0.5°C for one hour before a 0.15 gram of media was added. In order to maintain a constant pH during *kinetic* studies, the automatic titrator was installed in the reactor and connected with a pH electrode and small tubes running from two pumps, titrating with small volumes of acid (HNO_3, 0.01 *M*) and base (NaOH, 0.01 *M*) stock solution. One of the two pumps, connected to either the acid or base stock solution, was operated when the pH drifted ±0.02 pH units from the initial pH. An aliquot of 5 mL of suspensions was withdrawn at 2~60 minute intervals and filtered through a 0.45-μm Uniflo® filter unit for arsenate analysis. It was found that the pseudo-second order *kinetic* equation agreed with many adsorption processes using heterogeneous materials, of which chemisorptions are the rate-controlling step (Ho and McKay, 1998; Reddad *et al.*, 2002). Therefore, all of the *kinetic* data were fitted with a pseudo-second *kinetic* model to measure the rate constants, initial sorption rates, and adsorption capacities of arsenate.

Arsenate Adsorption *Isotherm* Tests

Granular activated alumina, SBA-15, and the most efficient lanthanum percentage, 50 percent, impregnated SBA-15 were used for *isotherm* tests. In this test, the initial arsenate concentration was fixed at 0.267 or 0.667 mmol/L, and masses of media were varied. A 50 mL of $NaNO_3$ (0.01 *M*) solution prepared with deionized water was poured into a polyethylene bottle. Then, arsenate stock solution and media were added to achieve target arsenate concentrations as well as the pH of the samples was adjusted to 7.2±0.02 with acid and base stock solutions while mixing with magnetic stirrer. All samples were mixed in a rotary shaker at 150 rpm and 20±0.5°C. After 8 hrs of shaking, the pH of the samples was readjusted to 7.2±0.02

with the pH automatic titrator using small volumes of acid and base stock solutions. All samples were then shaken in the rotary shaker until equilibrium state was reached. After 24 hrs of shaking, 5 mL was withdrawn and filtered with a 0.45-μm Uniflo® filter unit. All *isotherm* data were fitted with *Freundlich* and *Langmuir isotherm* models to evaluate several parameters.

Arsenic Analysis

A Varian AA-975 Atomic Absorption Spectrophotometer and a GTA-95 Graphite Tube Atomizer with programmable sample dispenser (Palo Alto, California) were used for arsenate analysis of samples. In this analysis, 20 mg/L nickel solution was used as a matrix modifier. The detection limit of AAS-graphite was 0.0474 μg/L.

1.3 RESULTS AND DISCUSSION

Conductivity tests

Figure 1 shows the conductivities of 80 percent lanthanum-impregnated SBA-15 calcined at different temperatures. As the calcinations temperature increased, the conductivities decreased because more lanthanum ions were oxidized as a result of the higher temperature. The conductivity of material calcined at 550°C was the same as that of deionized water, indicating the complete oxidation of lanthanum precursor. Therefore, all lanthanum-impregnated SBA-15 used in all subsequent experiments was synthesized using a final temperature of 550°C.

X-ray diffraction

Figure 2 (A) shows x-ray diffraction results of SBA-15 and various amounts of lanthanum-impregnated SBA-15 in the range of 0.8° and 2.1°. Calcined SBA-15 displayed a well-resolved pattern at very low 2θ with a sharp peak at 0.92° and two weak peaks at 1.60° and 1.84°. This x-ray diffraction pattern was similar to the reported SBA-15 pattern (Zhao *et al.*, 1998). The XRD peaks of SBA-15 can be indexed to a hexagonal lattice with a *d*(100) spacing of 95.93 Å, corresponding to a unit cell parameter a_0 of 110.78 Å obtained by the following equation: $a_0 = 2 \times d_{100} / \sqrt{3}$. With increase of lanthanum impregnation percentages onto SBA-15, the peak intensities at *d*(100) decreased gradually and the width of peak shapes broadened, indicating that a wide range of pore structures can be developed with increase of lanthanum impregnation (Nooney *et al.*, 2001). Figure 2 (B) shows the change of *d*(100) space with the increase of lanthanum-impregnated percentages. The *d*(100) space or unit cell parameter (a_0) of La_{10}SBA-15 was not different from calcined SBA-15. However, the *d*(100) spaces were linearly decreased to 89.33 Å (La_{50}SBA-15) with increase of lanthanum impregnation. Accordingly, lanthanum oxide was coated into mesopore structures of SBA-15 to have a smaller unit cell parameter. Sauer *et al.*(2002) also found a similar trend in their synthesis of europium doped yttria (YOX)-dispersed SBA-15. However, with increase to 80%, the *d*(100) space increased again to 91.94 Å. This phenomenon could be caused by an immoderate substitution of lanthanum into silica networks at 80 percent of lanthanum impregnation percentage. The increase of *d*(100) space or unit cell parameter by substitution of other metals into mesoporous silica has been observed by other researchers (Dapurkar and Selvam, 2001; Kuang *et al.*, 2001; Newalkar *et al.*, 2001b). A wide-angle of x-ray diffraction analysis was performed for highest amount (80 percent) of lanthanum-impregnated SBA-15 in this study. Figure 2 (C) shows the wide-angle of x-ray diffraction patterns for La_{80}SBA-15. For the x-ray diffraction of La_{80}SBA-15, even though the weight percentage of lanthanum element impregnated into SBA-15 was 44.4% in the solid (0.444 g (lanthanum)/g of media), there was no distinct peak; instead, very

weak and wide range of peaks were found in the range of 25~32°, indicating that nano-scale of lanthanum oxide was homogeneously dispersed into the mesopore structures of SBA-15 and no large size of lanthanum oxide particles were formed outside of SBA-15 (Sauer *et al.*, 2002; Yang *et al.*, 2003).

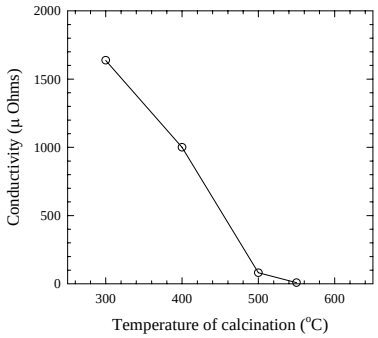

FIGURE 1 Conductivity tests of 80 percent lanthanum-impregnated SBA-15 treated with different calcination temperatures

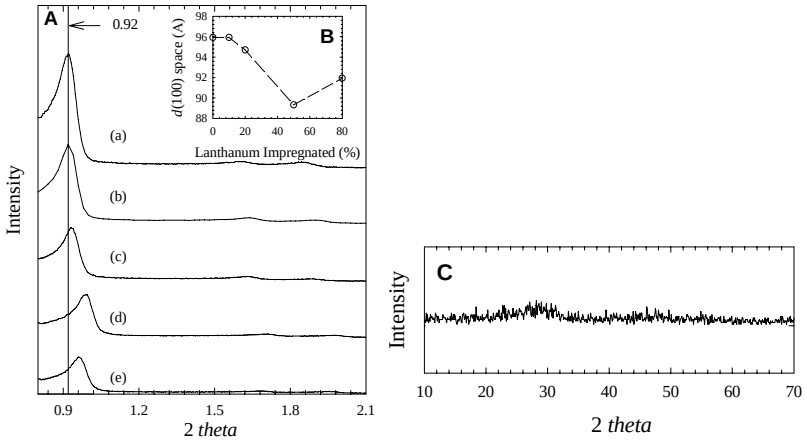

FIGURE 2 (A) Low-angle XRD measurements of SBA-15 (a), La_{10}SBA-15 (b), La_{20}SBA-15 (c), La_{50}SBA-15 (d), and La_{80}SBA-15 (e), (B) change of *d*(100) space with different lanthanum impregnation percentages, (C) a wide-angle of x-ray diffraction analysis performed for La_{80}SBA-15.

Nitrogen adsorption-desorption *isotherm*

Figure 3 (A) shows the nitrogen adsorption-desorption *isotherms* of calcined SBA-15 and various amounts of lanthanum-impregnated SBA-15. According to IUPAC (International Union of Pure and Applied Chemistry) classification, all *isotherms* show a typical Type IV model and have a H1 hysteresis loop, which is representative for mesopores (Sing *et al.*, 1985). The adsorbed volume of all *isotherms* sharply increased at relative pressure (P/P_0) of about 0.64, presenting capillary condensation of nitrogen within uniform mesopore structures (Kruk and Jaroniec, 1997). The inflection position of the relative pressure is related to a diameter in the mesopore range and the sharpness of these steps indicates the uniformity of the mesopore size distribution (Luan *et al.*, 1999; Newalkar *et al.*, 2001a). Up to 50 percent of lanthanum impregnation, the sharpness of inflection steps decreased gradually; however, it was largely declined at 80 percent. Also, inflection positions were slightly shifted toward lower relative pressure in the range of 0.4~0.8 with higher impregnation percentages of lanthanum. Therefore, it can be surmised that more heterogeneity of pore size distribution occurred for 80 percent

lanthanum-impregnated SBA-15 even though the exact change of mesopore diameters could not be detected from the nitrogen *isotherms*. To investigate the change of primary mesopore size distribution (PSD) with lanthanum impregnation, the KJS approach was conducted for the nitrogen *isotherms*. From the nitrogen *isotherms*, the PSD plots were derived from the adsorption branch of the nitrogen hysteresis because the network penetration effects of polyethylene oxide (PEO) chains of the triblock copolymer template within the silica framework of SBA-15 cannot fully be excluded on the desorption branch (Sauer *et al.*, 2002). Table 1 shows the physical parameters of nitrogen *isotherms* for all media such as BET surface area, total pore volume, micropore area and volume, primary mesopore area, volume, and size, as well as *d*(100) spacing (Å) and unit cell parameter (a_0, Å) obtained by XRD analysis. Except primary mesopore sizes and unit cell parameters, most parameters obtained from nitrogen *isotherms* decreased with increase in lanthanum impregnation percentages even though the decrease trends of each parameter were different. The reductions of primary mesopore surface area and volume indicate the formation of lanthanum oxides within mesopore structures (Morey *et al.*, 2000). As a special aspect, micropores of about 160 m^2/g were developed in the SBA-15 because there are some evidences of microporous corona effect resulted by the partial embedding of the PEO chains in the silica walls (Kruk *et al.*, 2000; Sauer *et al.*, 2002). The reduction of micropore and primary mesopore volumes of different amounts of lanthanum-impregnated SBA-15 is shown at Figure 3 (B). With 20 percent of lanthanum impregnation, micropore volume decreased significantly to 21 percent while primary mesopore volume decreased to 69.5 percent. Moreover, the primary mesopore volumes were linearly reduced from 10 percent to 80 percent lanthanum impregnation while micropore volume reductions were not much changed with higher lanthanum impregnation than 20 percent. Accordingly, micropore volume can be saturated with fewer amounts of lanthanum impregnation than primary mesopore. Overall results showed that most adsorption active surface sites of lanthanum-impregnated SBA-15 could exist at mesopore phase, excluding micro- and macro-pore structures. The pore size distribution of calcined SBA-15 and various amount of lanthanum-incorporated SBA-15 obtained from adsorption *isotherm* branches were shown in Figure 4. All media showed a sharp PSD. As shown in Figure 4, a broad maximum peak (73.1 Å) for SBA-15 was changed to be sharp and shifted to have a smaller maximum peak of 60.9 Å with 10 percent lanthanum impregnation even though the adsorbed volume of maximum peak was not much reduced. With increase in lanthanum impregnation up to 50 percent, the maximum peaks were more sharpened and their adsorbed volumes gradually decreased. When the lanthanum impregnation was increased to 80 percent, the maximum peak of PSD was changed again to be broadened and shifted to have a larger pore (63.1 Å) than that of 50 percent. Moreover, its adsorbed volume was abruptly decreased, representing more heterogeneous pore structures than other media. The increase in primary mesopore size might be linked with the increase of *d*(100) shown with XRD analysis, which can be caused by the fact that lanthanum precursors are substituted into silicon to expand the unit cell at 80 percent of lanthanum impregnation.

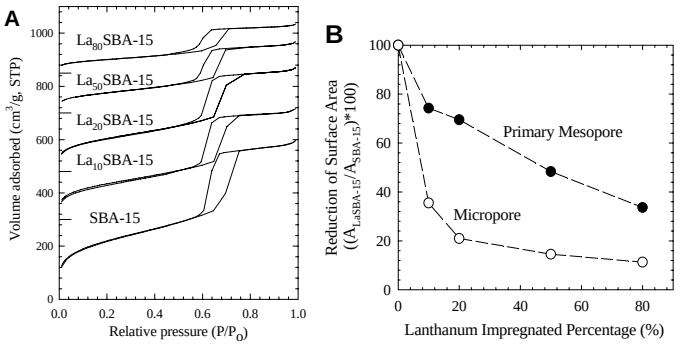

FIGURE 3 (A) Nitrogen adsorption-desorption *isotherms* of SBA-15, La_{10}-, La_{20}-, La_{50}-, and La_{80}SBA-15, (B) Reductions of primary mesopore and micropore volumes according to lanthanum impregnation percentages

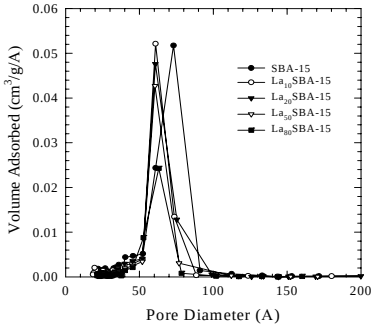

FIGURE 4 Pore size distributions of La_{80}SBA-15, La_{50}SBA-15, La_{20}SBA-15, La_{10}SBA-15, and SBA-15 obtained from adsorption branches

Fourier Transform Infrared (FTIR) Spectroscopy Analysis

Figure 5 (A) shows the IR spectra of uncalcined and calcined La_{20}SBA-15. The strong peaks in the IR band of 1250~1700 cm^{-1} of uncalcined La_{20}SBA-15 disappeared completely for calcined La_{20}SBA-15. The vibration mode of nitrate can be broadly assigned for the IR band of 1650~750 cm^{-1}, especially a number of peaks in the NO_2 stretching region of 1250~1700 cm^{-1} suggests the presence of nitrate ions (Klingenberg and Vannice, 1996). From this result, it is concluded that nitrate ions of lanthanum precursor were totally decomposed with a calcination procedure employed. Figure 5 (B) shows the IR patterns of calcined SBA-15, LaSBA-15, and lanthanum oxide in the wave number of 400~1600 cm^{-1}. The three peaks at 465 cm^{-1}, 800 cm^{-1}, and 1085 cm^{-1} corresponded to rocking, bending (or symmetric stretching) and asymmetric stretching of the intertetrahedral oxygen atoms in the SiO_2 structure, respectively, for the IR patterns of calcined SBA-15 (Primeau *et al.*, 1997; Morey *et al.*, 2000). The peak at 960 cm^{-1} was also assigned to the stretching of nonbridging oxygen atoms ($Si\text{-}O^{\delta-}$) of a Si-OH stretch (Morey *et al.*, 2000). The peaks of 1085 cm^{-1} and the shoulder part in the IR bands of 1100~1300 cm^{-1} corresponded to the concerted (Si-O-Si) stretches, which were as a result of partial ordering of the silicate framework at the pore surface (Morey *et al.*, 2000). With an increase of lanthanum-impregnated percentages up to 20 percent, there were no peaks in the IR band of 1300~1600 cm^{-1}, exhibiting the phase of lanthanum oxide (La-O-La), although the absorbance intensities of 960 cm^{-1} decreased, implying that Si-OH groups were consumed to transform to Si-O-La bonds. From this result, it can be suggested that the monolayer phase of lanthanum oxide might be dominated at 20 percent of lanthanum impregnation. At 50 percent of lanthanum impregnation, however, the peak of 960 cm^{-1} disappeared completely, but the very small peaks in the IR band

of 1300~1600 cm^{-1} appeared, indicating that more lanthanum precursors than needed for a complete consumption of Si-OH were involved for the multilayer of La-O-La bonds. Therefore, the multilayer phase of lanthanum oxide might be dominated at 50 percent lanthanum impregnation. It can be concluded from the above facts that the silanol groups on SBA-15 served as active sites for lanthanum incorporation and were consumed. With higher lanthanum impregnation than 50 percent, the IR peaks of 1300~1600 cm^{-1} were increased more , showing the lanthanum oxide phase clearly, which was also observed by other researchers (Klingenberg and Vannice, 1996). Even at the highest impregnation percentage (80 percent) of lanthanum, however, the IR peak of 1085 cm^{-1} and shoulder part in the IR bands of 1100~1300 cm^{-1} did not decrease. Accordingly, it can be surmised from this result that there was no structural collapse of pore structures occurred by the attacks of lanthanum precursors for Si-O bonds of mesoprous frameworks although a partial substitution of lanthanum with silicon occurred at 80 percent as proved by XRD and PSD analysis. For the case of aluminum impregnation (Shin *et al.*, 2003) in our study, the declinations of 1085 cm^{-1} and shoulder part in the IR bands of 1100~1300 cm^{-1} were distinctly occurred at 30 percent of aluminum impregnation. The structural collapse was also proved by XRD, PSD, and TEM analysis. In the *kinetic* studies of phosphate adsorption by use of aluminum impregnated SBA-15, much lower adsorption capacity was achieved at 30 percent of aluminum impregnation (Shin *et al.*, 2003). Therefore, structural collapse seems to be a significant factor for hindering the arsenate adsorption. Surprisingly, lanthanum was a good candidate of functioning materials for the mesoporous silicate supports in terms of structural stability as shown by other studies (Kloetstra *et al.*, 1997; Zhang and Pinnavaia, 1998; Melo and Urquieta-Gonzalez, 2001).

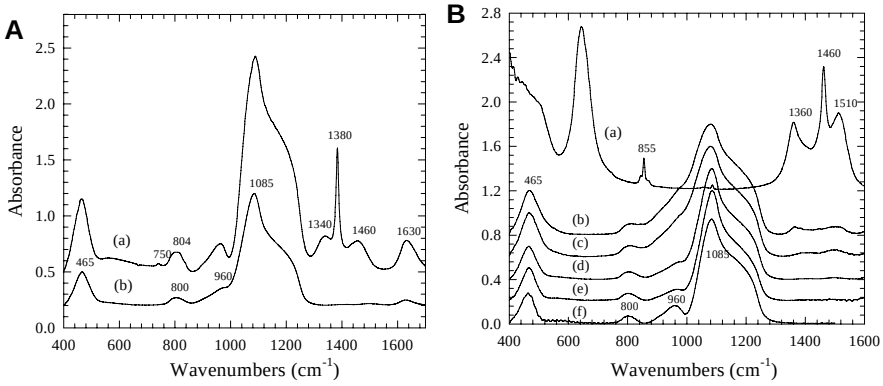

FIGURE 5 (A) FTIR spectra of uncalcined La_{20}SBA-15 (a) and calcined La_{20}SBA-15 (b), (B) FTIR spectra of lanthanum oxide (a), La_{80}SBA-15 (b), La_{50}SBA-15 (c), La_{20}SBA-15 (d), La_{10}SBA-15 (e), and SBA-15 (f)

Kinetic Studies of Arsenate Adsorption

Figure 6 (A) shows the arsenate adsorption *kinetics* of activated alumina and various amounts of lanthanum-impregnated SBA-15 as well as their fitting curves of pseudo-second order *kinetic* model. In comparison with activated alumina, more rapid and higher sorption capacities were obtained even at 10 percent lanthanum-impregnated SBA-15. Higher adsorption capacities were achieved; longer equilibrium times were taken for all *kinetics*. Since the q_{eq} values obtained by the pseudo-second order *kinetic* model were overestimated due to a few data of more extended time than 400 minutes and a trend of adsorption capacities was similar to the trend of arsenate adsorption capacities at 400 minutes (designated to $q_{(t=400)}$), the initial sorption rate (v_0) and $q_{(t=400)}$ values in accordance with the lanthanum impregnation percentages were

expressed in Figure 6 (B). The $q_{(t=400)}$ values linearly increased to 1.66 $mmol_{As}/g$ (124.4 mg_{As}/g) with an increase of lanthanum impregnation up to 50%, but slightly decreased to 1.54 $mmol_{As}/g$ (115.4 mg_{As}/g) at 80 percent while the initial sorption rate sharply increased to 0.016 $mmol \cdot g^{-1} \cdot min^{-1}$ at 20 percent and further increased to 0.023 $mmol \cdot g^{-1} \cdot min^{-1}$ at 50 percent, but decreased to 0.020 $mmol \cdot g^{-1} \cdot min^{-1}$ at 80 percent. Figure 6 (C) shows the changes of arsenate adsorption densities and surface loadings with an increase of lanthanum impregnation percentages. The arsenate surface loading linearly increased as the lanthanum impregnation percentages increased while arsenate adsorption densities increased up to 50 percent of lanthanum impregnation, however, abruptly decreased at 80 percent impregnation. Correspondingly, there was a most efficient amount of lanthanum impregnation percentage that had the maximum arsenate adsorption capacity by increase of active sorption sites although the surface area of media decreased with increase of lanthanum impregnation. However, the occurrence of substitution with silicon in addition to the reduction of surface area might give a significant hindrance of arsenate adsorption capacity since a partial portion of lanthanum immobilized at the silica framework will not be functioning as active sorption sites for arsenate removal and the exchanged silicon can obstruct the active sites of lanthanum. Therefore, despite of the fact that a larger lanthanum was impregnated in SBA-15 than 50 percent, the reason for the decrease in the overall adsorption capacity of La_{80}SBA-15 might be due to not only a decrease of surface area but also silicon substitution, which were proved by the XRD and N_2 gas *isotherm* analysis. As a result of *kinetic* studies, the most efficient percentage of lanthanum impregnation was 50 percent in terms of arsenate adsorption speed and capacity. La_{50}SBA-15 also had about 10, 38, and 13 times higher $q_{(t=400)}$ ($mmol_{As}/g$), arsenate adsorption density ($mmol_{As}/mmol_{Me}$), and surface loading ($mmol_{As}/m^2$), respectively, than activated alumina. Although the active sites of activated alumina might be larger than that of La_{50}SBA-15 due to a larger surface area, it can be surmised by the following explanation that the lanthanum oxide incorporated SBA-15 was much more active than activated alumina in terms of physical and chemical properties. First, a large number of active sites for arsenate removal were achieved by the nano-scale dispersion of lanthanum precursors onto a highly ordered mesopore structures. Second, since most lanthanum active sites of SBA-15 exists in a relatively uniform hexagonal-open mesopore size distribution excluding micro- and macro-pores, the arsenate accessibility of lanthanum-impregnated SBA-15 was much better than that of activated alumina that has amorphorous matrices of aluminum oxides containing bottleneck shapes of pore structures hindering the accessibility of arsenate molecules to the active sites of the media (Kim, 2001).

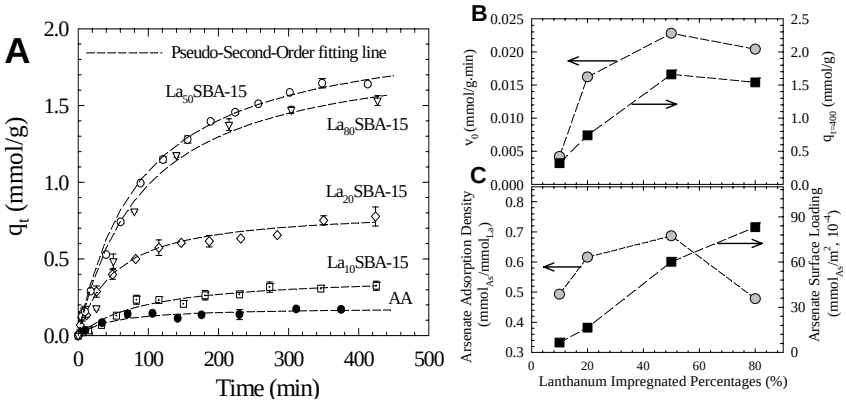

FIGURE 6 (A) Arsenate Adsorption *Kinetics* with LaSBA-15 and activated alumina (AA-400G, ALCAN®) (pH 7.2±0.02), (B) Initial sorption rate (v_0) and q_{eq} ($mmol_{As}/g$), (C) Arsenate adsorption density and surface loading.

Arsenate Adsorption *Isotherms* with LaSBA-15

Figure 7 shows the arsenate adsorption *isotherms* of activated alumina, SBA-15, and La_{50}SBA-15 at an initial arsenate concentration of 0.267 or 0.667 $mmol_{As}/L$. At an initial arsenate concentration of 0.267 mmol/L, SBA-15 and activated alumina had arsenate adsorption capacities of less than 0.06 and 0.12 mmol/g, respectively, while La_{50}SBA-15 (about 1.2 mmol/g) showed about 20 and 10 times higher adsorption capacities than SBA-15 and activated alumina, respectively. Therefore, the lanthanum oxide species incorporated onto the mesopore phase of SBA-15 were the most dominated active sorption sites for arsenate removal. Moreover, as similar to the magnification of adsorption capacities for both La_{50}SBA-15 and activated alumina in *kinetic* studies, La_{50}SBA-15 showed much more active sorption capacities than activated alumina, although absolute values of *isotherms* were different with those of *kinetics* due to a different experimental setup. With an increase in initial arsenate concentration, the adsorption capacity of La_{50}SBA-15 increased to about 1.6 $mmol_{As}/g$ (119.9 mg_{As}/g) at 0.11 $mmol_{As}/L$. In spite of the fact that any mechanistic implication cannot be obtained from the determination coefficients of both *Langmuir* and *Freundlich* models because both models had very similar determination coefficients (Table 1) (Sposito, 1984), the q_{max} values of *Langmuir* model were used to get the values of arsenate adsorption density ($mmol_{As}/mmol_{La}$) and arsenate surface loading ($mmol_{As}/m^2$, BET). La_{50}SBA-15 showed about 9, 34, and 12 times higher for q_{max} ($mmol_{As}/g$), arsenate adsorption density ($mmol_{As}/mmol_{Me}$), and surface loading ($mmol_{As}/m^2$), respectively, than activated alumina, demonstrating a consistency with previous *kinetic* results. In Table 3, *isotherm* results of La_{50}SBA-15 were compared with other studies in which lanthanum was impregnated onto an alumina (Wasay *et al.*, 1996b) or silica gel (Wasay *et al.*, 1996a). Although the results of other studies showed no interference of other anions such as Cl^-, Br^-, I^-, NO_3^-, and SO_4^{2-} for arsenate removal, the adsorption capacity (1.651 $mmol_{As}/g$) of La_{50}SBA-15 obtained at lower arsenate concentration (0.667 $mmol_{As}/L$) in this study was about 10 or 14 times higher than the referenced values of La(III) impregnated alumina (0.172 $mmol_{As}/g$) or La(III) impregnated silica gel (0.118 $mmol_{As}/g$) at 1 $mmol_{As}/L$ or 0.5~2 $mmol_{As}/L$ of initial arsenate concentations, respectively. Accordingly, the nano-scale impregnation of lanthanum onto SBA-15 has a lot of advantages in terms of not only adsorption velocity and capacity but also cost benefits for small scale of POU/POE application of arsenate removal since a small amount of lanthanum precursor is needed for impregnation and the regeneration of the

lanthanum-impregnated mesoporous media will be applicable due to excellent structural stability of lanthanum-impregnated SBA-15.

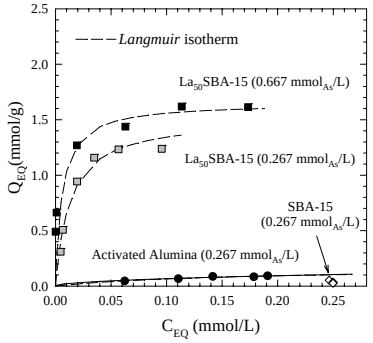

FIGURE 7 Arsenate Adsorption *Isotherm* of La_{50}SBA-15 and activated alumina (AA-400G, ALCAN®) at 0.267 $mmol_{As}$/L or 0.667 $mmol_{As}$/L of arsenate initial concentrations.

TABLE 1 Determination Coefficients (R^2), Several Parameters for the Fit of Arsenate Adsorption Isotherm Data to Both Freundlich and Langmuir Isotherms, and Comparison with Other Studies

Adsorption *isotherms* and parameters		This study			References	
		Activated alumina	La_{50}SBA-15		La(III)- alumina[c]	La(III)- silica gel[d]
As(V) conc. (mmol/L)		0.267	0.267	0.667	1	0.5~2
Langmuir	*b* (L/mmol)	5.98	77.52	167.37	19.7	-
	q_{max} (mmol/g)	0.172	1.516	1.651	0.172	0.118
	q_{max}[a]	0.019	0.63	0.68	–	–
	q_{max}[b]	4.9~4.5	54.9	59.8	56.8	4.03
	BET (m^2/g)	350~380[g]	276	276	45.1	293
	R^2	0.976	0.993	0.922	-	-

[a] arsenate adsorption density ($mmol_{As}/mmol_{Me}$), [b] surface loading ($mmol/m^2$) ($\times 10^{-4}$), [c] lanthanum(III) impregnated alumina (Wasay *et al.*, 1996b), [d] Lanthanum (III) impregnated silica gel (Wasay *et al.*, 1996a), [g] obtained from the reference (ALCAN, 1997).

CONCLUSIONS AND RECOMMENDATIONS

Although the lanthanum oxide was highly dispersed into the mesopore structures of SBA-15 without producing lanthanum oxide particles at 80%, a partial substitution of lanthanum into silica networks was observed by XRD and N_2 gas *isotherm*. According to a result of FTIR, however, there was no structural collapse of silica frameworks at 80 percent since a partial of lanthanum precursors substituted with silicon might play an important role of structural stabilization as has been proved at other studies. In the arsenate adsorption kinetics, due to the partial substitution of lanthanum at 80 percent, the arsenate adsorption densities abruptly decreased at 80 percent., leading to the overall reduction of arsenate adsorption capacity. The most efficient impregnated percentage, 50 percent, was used for arsenate isotherms tests. Therefore, lanthanum impregnated SBA-15 can be used to remove arsenic in groundwater effectively.

1.4 REFERENCES

Adutwum, K. O.; Adsorption Mechanism of Oxyanions of Selenium on to Lanthanum Oxide and Alumina. University of Reno: Reno, Nev., 1995.

ALCAN; Alcan Chemicals (Product Data, Activated Aluminas), 1997.

Dapurkar, S. E.; Selvam, P.; Encapsulation of Fe2O3 Nanoparticles in Periodic Mesoporous Materials. Mater. Phys. Mech., 2001; Vol. 4, pp 13-16.

Fryxell, G. E.; Liu, J.; Hauser, T. A.; Nie, Z.; Ferris, K. F.; Mattigod, S.; Gong, M.; Hallen, R. T.; Design and Synthesis of Selective Mesoporous Anion Traps. Chem. Mater., 1999; Vol. 11, pp 2148-2154.

Ho, Y. S.; McKay, G.; A Comparison of Chemisorption Kinetic Models Applied to Pollutant Removal on Various Sorbents. Trans IChemE, 1998; Vol. 76B, pp 332-340.

Jang, M.; Shin, E. W.; Park, J. K.; Choi, S. I.; Mechanisms of Arsenate Adsorption by Highly-Ordered Nano-Structured Silicate Media Impregnated with Metal Oxides. Accepted in Environmental Science and Technology, 2003.

Kim, Y. S.; Characteristics of γ-Alumina Prepared from Rehydrated Amorphous Alumina. Kor. J. Mat. Res., 2001; Vol. 11, pp 957-965.

Klingenberg, B.; Vannice, M. A.; Influence of Pretreatment on Lanthanum Nitrate, Carbonate, and Oxide Powders. Chem. Mater., 1996; Vol. 8, pp 2755-2768.

Kloetstra, K. R.; Laren, M. V.; Bekkum, H. V.; Binary Caesium-Lanthanum Oxide Supported on MCM-41: A New Stable Heterogeneous Basic Catalyst. J. Chem. Soc., Faraday Trans., 1997; Vol. 93, pp 1211-1220.

Kruk, M.; Jaroniec, M.; Application of Large Pore MCM-41 Molecular Sieves to Improve Pore Size Analysis Using Nitrogen Adsorption Measurements. Langmuir, 1997; Vol. 13, pp 6267-6273.

Kruk, M.; Jaroniec, M.; Ko, C. H.; Ryoo, R.; Characterization of the Porous Structure of SBA-15. Chem. Mater., 2000; Vol. 12, pp 1961-1968.

Kuang, Y.; He, N.; Wang, J.; Xiao, P.; Yuan, C.; Lu, Z.; Investigating the State of Fe and La in MCM-41 Mesoporous Molecular Sieve Materials. Colloids and Surfaces A: Physicochemical and Engineering Aspects, 2001; Vol. 179, pp 177-184.

Luan, Z.; Maes, E. M.; Van der Heide, M. A. W.; Zhao, D.; Czernuszewicz, R. S.; Keven, L.; Incorporation of Titanium into Mesoporous Silica Molecular Sieve SBA-15. Chem. Mater., 1999; Vol. 11, pp 3680-3686.

Lukens, W. W.; Schmidt-Winkel, P.; Zhao, D.; Feng, J.; Stucky, G. D.; Evaluating Pore Sizes in Mesoporous Materials: A Simplified Standard Adsorption Method and a Simplified Broekhoff-de Boer Method. Langmuir, 1999; Vol. 15, pp 5403-5409.

Melo, R. A. A.; Urquieta-Gonzalez, E. A.; The Influence of Al, La or Ce in the Thermal and Hydrothermal Properties of MCM-41 Mesoporous Solids. In Zeolites and mesoporous materials at the dawn of the 21st century: proceedings of the 13th International Zeolite Conference: Montpellier, France, 2001.

Misra, M.; Nayak, D. C.; Process for Removal of Selenium and Arsenic from Aqueous Streams. In US Patent No 5,603,838, 1995.

Morey, M. S.; O'Brien, S.; Schwarz, S.; Stucky, G. D.; Hydrothermal and Postsynthesis Surface Modification of Cubic, MCM-48, and Ultralarge Pore SBA-15 Mesoporous Silica with Titanium. Chem. Mater., 2000; Vol. 12, pp 898-911.

Newalkar, B. L.; Olanrewaju, J.; Komarneni, S.; Direct Synthesis of Titanium-Substituted Mesoporous SBA-15 Molecular Sieve under Microwave-Hydrothermal Conditions. Chem. Mater., 2001a; Vol. 13, pp 552-557.

Newalkar, B. L.; Olanrewaju, J.; Komarneni, S.; Microwave-Hydrothermal Synthesis and Characterization of Zirconium Substituted SBA-15 Mesoporous Silica. J. Phys. Chem. B, 2001b; Vol. 105, pp 8356-8360.

Nooney, R. I.; Kalyanaraman, M.; Kennedy, G.; Maginn, E. J.; Heavy Metal Remediation Using Functionalized Mesoporous Silicas with Controlled Macrostructure. Langmuir, 2001; Vol. 17, pp 528-533.

Primeau, M.; Vautey, C.; Langlet, M.; The effect of thermal annealing on aerosol-gel deposited SiO_2 films: a FTIR deconvolution study. Thin Solid Films, 1997; Vol. 310, pp 47-56.

Reddad, Z.; Gerente, C.; Andres, Y.; Le Cloirec, P.; Adsorption of Several Metal Ions onto a Low-Cost Biosorbent: Kinetic and Equilibrium Studies. Environmental Science & Technology, 2002; Vol. 36, pp 2067-2073.

Sauer, J.; Marlow, F.; Spliethoff, B.; Schuth, F.; Rare Earth Oxide Coating of the Walls of SBA-15. Chem. Mater., 2002; Vol. 14, pp 217-224.

Shin, E. W.; Han, J. S.; Jang, M.; Min, S.-H.; Park, J. K.; Rowell, R. M.; Phosphate Adsorption on Al-Impregnated Mesoporous Silicate: Surface Structure and Adsorption Behavior. submitted to Environmental Science and Technology, 2003.

Sing, K. S. W.; Everett, D. H.; Haul, R. A. W.; Moscow, L.; Pierotti, R. A.; Rouquerol, J.; Siemieniewska, T.; Reporting Physisorption Data for Gas/solid Systems with Special Reference to the Determination of Surface Area and Porosity. Pure Appl. Chem., 1985; Vol. 57, pp 603-619.

Sposito, G.; Oxford University Press: New York, 1984.

Tokunaga, S.; Hakuta, T.; Wasay, S. A.; Treatment of Waters Containing Hazardous Anions Using Rare-Earth Based Materials. Journal of the National Institute of Materials and Chemical Research, 1999a; Vol. 7, pp 291-334.

Tokunaga, S.; Wasay, S. A.; Park, S. W.; Removal of Arsenic(V) Ion From Aqueous Solutions by Lanthanum Compounds. Water Science and Technology, 1997; Vol. 35, pp 71-78.

Tokunaga, S.; Yokoyama, S. A.; Wasay, S. A.; Removal of Arsenic (III) and Arsenic (V) Ions from Aqueous Solutions with Lanthanum (III) Salt and Comparison with Aluminum (III), Calcium (II), and Iron (III) Salts. Water Environment Research, 1999b; Vol. 71, pp 299-306.

Wasay, S. A.; Haron, M. J.; Tokunaga, S.; Adsorption of fluoride, phosphate, and arsenate ions on lanthanum-impregnated silica gel. Water Environment Research, 1996a; Vol. 68, pp 295-300.

Wasay, S. A.; Tokunaga, S.; Park, S. W.; Removal of Hazardous Anions from Aqueous Solutions by La(III)- and Y(III)-Impregnated Alumina. Separation Science and Technology, 1996b; Vol. 31, pp 1501-1514.

Yang, C. M.; Liu, P. H.; Ho, Y. F.; Chiu, C. Y.; Chao, K. J.; Highly Dispersed Metal Nanoparticles in Functionalized SBA-15. Chem. Mater., 2003; Vol. 15, pp 275-280.

Yoshitake, H.; Yokoi, T.; Tatsumi, T.; Adsorption of Chromate and Arsenate by Amino-Functionalized MCM-41 and SBA-1. Chem. Mater., 2002; Vol. 14, pp 4603-4610.

Yoshitake, H.; Yokoi, T.; Tatsumi, T.; Adsorption Behavior of Arsenate at Transition Metal Cations Captured by Amino-Functionalized Mesoporous Silicas. Chem. Mater., 2003; Vol. 15, pp 1713-1721.

Zhang, W.; Pinnavaia, T. J.; Rare Earth Stabilization of Mesoporous Alumina Molecular Sieves Assembled Through an N^oI^o Pathway. Chem. Commun., 1998; Vol. 11, pp 1185-1186.
Zhao, D.; Feng, J.; Huo, Q.; Melosh, N.; Fredrickson, G. H.; Chmelka, B. F.; Stucky, G. D.; Triblock Copolymer Syntheses of Mesoporous Silica with Periodic 50 to 300 Angstrom Pores. SCIENCE, 1998; Vol. 279, pp 548-552.

1.5 APPENDIX A:

- **SCI Paper**

(1) Min Jang, Eun Woo Shin, Jae K. Park, and Sang I. Choi, Mechanisms of Arsenate Adsorption by Highly-Ordered Nano-Structured Silicate Media Impregnated with Metal Oxides, Accepted in *Environmental Science and Technology* (August 28, 2003).

(2) Eun Woo Shin, James S. Han, Min Jang, Soo-Hong Min, Jae Kwang Park, and Roger M. Rowell, Phosphorus Adsorption on Al-Impregnated Mesoporous Silicate: Surface Structure and Adsorption Behavior, Submitted to *Environmental Science and Technology*.

(3) Min Jang, Park, J. K., Eun Woo Shin, Lanthanum Functionalized Highly Ordered Mesoporous Media for Arsenic Removal, Submitted to *Environmental Science and Technology*.

- **US Patent**

Jae K. Park and Min Jang, "Removal of Arsenic and Other Anions Using Novel Adsorbents," Patent (U.S. Patent) proceeding

- **Presentation**

Min Jang, Eun Woo Shin, and Jae K. Park, Removal of Arsenic Using Mesoporous Silicate Media Impregnated Metal Oxides Nano-Particles, WEFTEC, Research Section 41, Chicago.

1.6 APPENDIX B:

(1) Eun Woo Shin, James S. Han, Min Jang, Soo-Hong Min, Jae Kwang Park, and Roger M. Rowell, Phosphorus Adsorption on Al-Impregnated Mesoporous Silicate: Surface Structure and Adsorption Behavior, submitted to *Environmental Science and Technology*.